Available online at www.sciencedirect.com
ScienceDirect
Journal of Organometallic Chemistry 693 (2008) 475–482
Journal of Organometallic Chemistry
www.elsevier.com/locate/jorganchem

Theoretical studies on the imine germylenoid HN=GeNaF and its insertion reaction with R–H (R = F, OH, NH_2, CH_3)

Xiaojun Tan [a,*], Weihua Wang [b], Ping Li [b], Qiufen Wang [a], Gengxiu Zheng [a], Fei Liu [c]

[a] College of Chemistry and Chemical Engineering, University of Jinan, Jinan, Shandong 250022, People's Republic of China
[b] Department of Chemistry, Qufu Normal University, Qufu, Shandong 273165, People's Republic of China
[c] Shandong Provincial Institute for Drug Control, Jinan, Shandong 250012, People's Republic of China

Received 13 September 2007; received in revised form 10 November 2007; accepted 13 November 2007
Available online 21 November 2007

Abstract

The geometries and isomerization of the imine germylenoid HN=GeNaF as well as its insertion reactions with R–H (R = F, OH, NH_2, CH_3) have been systematically investigated at the B3LYP/6-311+G* level of theory. The potential barriers of the four insertion reactions are 117.2, 172.6, 219.7, and 322.3 kJ/mol, respectively. Here, all the mechanisms of the four reactions are identical to each other, i.e., an intermediate has been formed first during the insertion reaction. Then, the intermediate could dissociate into the substituted germylene (HN=GeHR) and NaF with a barrier corresponding to their respective dissociation energies. Correspondingly, the reaction energies for the four reactions are 185.0, 208.1, 224.4, and 266.9 kJ/mol, respectively, which are linearly correlated with the calculated barrier heights. Compared with the insertion reaction of HN=Ge: and R–H, the introduction of NaF makes the insertion reaction occur easily though it is more difficult to proceed than that of insertion reaction between H_2GeNaF and R–H. Furthermore, the effects of halogen (F, Cl, Br) substitution and inorganic salts employed on the reaction activity have also been discussed. As a result, the relative reactivity among the four insertion reactions should be as follows: H–F > H–OH > H–NH_2 > H–CH_3.

Keywords: Imine germylenoid (HN=GeNaF); Insertion reaction; Density functional theory (DFT)

1. Introduction

Germylene is an important active intermediate in some organic germanium reactions. Some special reactions involving germylene, such as insertion reactions [1–4], addition reactions [5], polymerization reactions [6], and have been regarded as effective methods to synthesize relevant germanium compounds containing new bonds and heterocycles [7–9]. Moreover, the reactions of germylenes are of interest both because of their involvement in the breakdown mechanism of germanes leading to solid germanium (chemical vapor deposition) [10,11] and also because of their involvement in germane and organogermane decompositions [12]. Experimentally, several stable germylenes compounds have been synthesized [13–15]. The first direct kinetic measurements of germylene, GeH_2, have been reported by Becerra et al. [16] using the technique of laser flash photolysis combined with time-resolved laser resonant absorption. Employing the similar technology, more germylenes and their reactions have been studied in detail [17–20]. Therefore, the research of germanium reactions is an interesting topic since many organic germanium compounds have been found to have biologic activity [21–23]. As to the theoretical study of germylenes, some groups have reported the reaction of germylenes with small molecules, such as ethylene [24], quinine [25], oxirane, and thiirane [26]. The relative stabilities of germanitriles and germaimines have been systematically investigated and found that fluorine substitution can dramatically stabilize FGe≡N with respect to Ge=NF both from a kinetic and a thermodynamic viewpoint [27].

* Corresponding author.
E-mail address: chm_tanxj@ujn.edu.cn (X. Tan).

0022-328X/$ - see front matter © 2007 Elsevier B.V. All rights reserved.
doi:10.1016/j.jorganchem.2007.11.019

Similar to carbenoid and silylenoid, germylenoid is the complex formed between the germylene and inorganic salt, which can be denoted as R_1R_2GeMX (M = alkali metal, X = halogen) and may be stable than germylene and have particular property. There are some studies on germylenoid increasingly after Gaspar put forward to that germylenoid is intermediates in some chemical reactions [28]. For example, the geometries and reactions involving germylenoids H_2GeLiF [29] and H_2GeNaF [30] have been investigated theoretically. The unsaturated germylenoids $R_1R_2C{=}GeMX$ are another kind of germylenoids. At present, their existence, structures, and chemical properties have not been studied experimentally. Recently, Li et al. have studied the geometries and isomerization reaction of unsaturated germylenoid $H_2C{=}GeNaF$ theoretically [31]. Similarly, imine germylenoid HN=GeMX is one of the simplest unsaturated germylenoids, which is the complex of imine germylene HN=Ge: and MX (M = Li, Na, X = F, Cl). Imine germylene have been first characterized indirectly using various trapping reagents [32], and have been reported both experimentally [33,34] and theoretically [35,36] in recent years. However, relevant geometries of imine germylenoid and its reaction activities with R–H type molecules are still lack. In this paper, the imine germylenoid has been selected and its structures, stability, and insertion reaction with R–H (R = F, OH, NH_2, and CH_3) have been systematically investigated employing the mostly used B3LYP method within the framework of density functional theory (DFT). Considering the important role of general inorganic salts, such as LiF and NaF, in the insertion reactions, the HN=GeNaF as well as its insertion reaction has also been mainly discussed aiming to understand its relative activities compared with the system of germylenoid of H_2GeNaF [30]. At the same time, the influences of different inorganic salts and halogen substitution on the reaction activities have also been evaluated to fill the void of the available data for imine germylenoid. Hopefully, the present results would be helpful for further experimental and theoretical studies on germylenoids.

2. Calculation method

The popular hybrid density functional B3LYP method, namely Becke's three-parameter non-local exchange functional [37] with the non-local correlation functional of Lee et al. [38], and 6-311+G* basis set including diffuse and polarization functions have been employed comprehensively. The B3LYP/6-311+G* level of theory has been proved relatively accurate to treat with the relevant insertion reactions in our previous study [39]. To further evaluate the validity of it, the relevant HN=GeNaF complexes have been calculated using the advanced MP2/6-311+G* level of theory. Overall, both levels of theory can give the parallel results consistently. Considering the compromise between computational cost and accuracy and especially for comparison with the H_2GeNaF system on the same benchmark, the results of B3LYP/6-311+G* level of theory have been discussed below if not noted otherwise. Subsequently, frequency analyses have been carried out to confirm the nature of the minima and transition states. Moreover, intrinsic reaction coordinate (IRC) calculations have also been performed to further validate the calculated transition states connecting reactants and products. Additionally, relevant energy quantities, such as reaction energy and barrier energies, have been corrected with zero-point vibrational energy (ZPVE) corrections.

All the calculations have been performed using GAUSSIAN98 programs [40].

3. Results and discussion

Similar to the unsaturated germylene $H_2C{=}Ge$: [37], the most stable imine germylene HN=Ge: is also in singlet, where the singlet state is more favorable about 267.5 kJ/mol in energy relative to that of triplet state at the B3LYP/6-311+G* level of theory. Thus, the singlet state of HN=Ge: has been discussed in the following study. As displayed in Fig. 1, Ge and N atom adopt sp hybridization, where one of sp hybridization orbitals of Ge forms σ bond with N atom and two electrons of Ge occupy the other sp hybridization orbital. As for the two vertical p orbitals of Ge atom, one forms π bond with the corresponding p orbital of N and the other is the empty orbital without electron. Obviously, the empty p orbital and the sp hybridization orbital in Ge atom have electrophilicity and nucleophilicity, respectively. Expectedly, the complexation between the double functionality of Ge atom and the strong polar inorganic salts (e.g., NaF and LiF) should lead to the different complexes. As a result, full geometry optimizations suggest that three stable equilibrium structures for HN=GeNaF directly associated with the Ge atom have been located as well as two transition states connecting them (in Fig. 2). Correspondingly, the complexation processes of three stable complexes are schematically displayed in Fig. 3.

3.1. Structures and relative stabilities of HN=GeNaF

As displayed in Fig. 2, complex **1** is characterized by a four-membered ring structure, where all atoms lie in the same plane (C_s symmetry). Obviously, as shown in Fig. 3, complex **1** was formed when lone pairs of F^- in NaF molecule transfers to the empty sp-orbital of Ge accompanying the electron transfer from N to Na^+. Here,

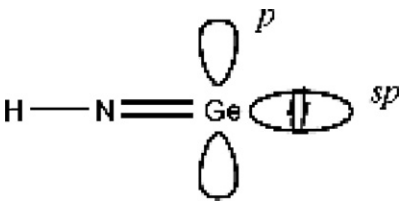

Fig. 1. Schematic diagram of singlet germylene HN=Ge:.

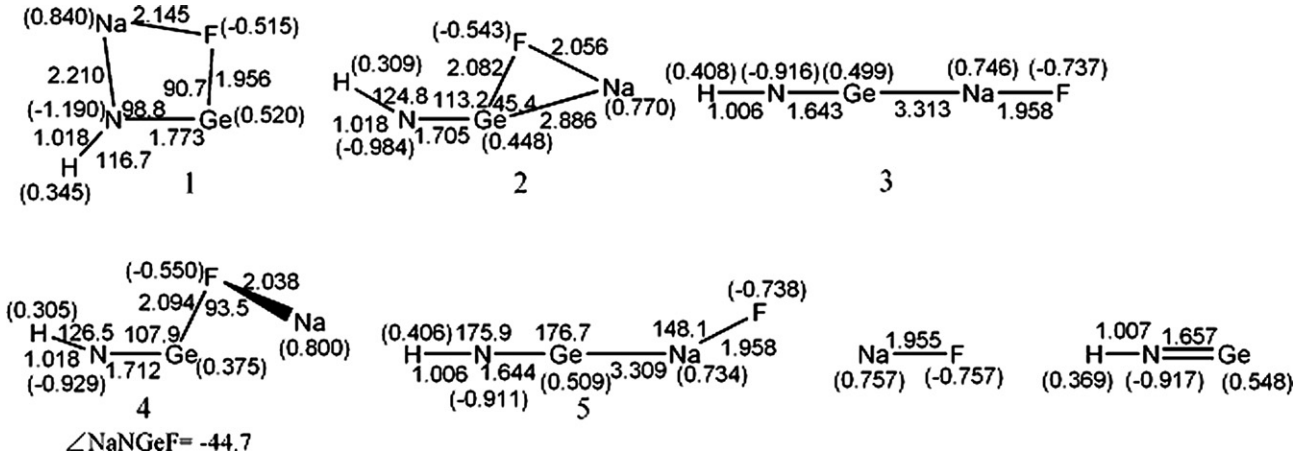

Fig. 2. The geometries of HN=GeNaF, where the bond length and bond angel are in angstrom and degree, respectively. Values in parentheses are the natural charges.

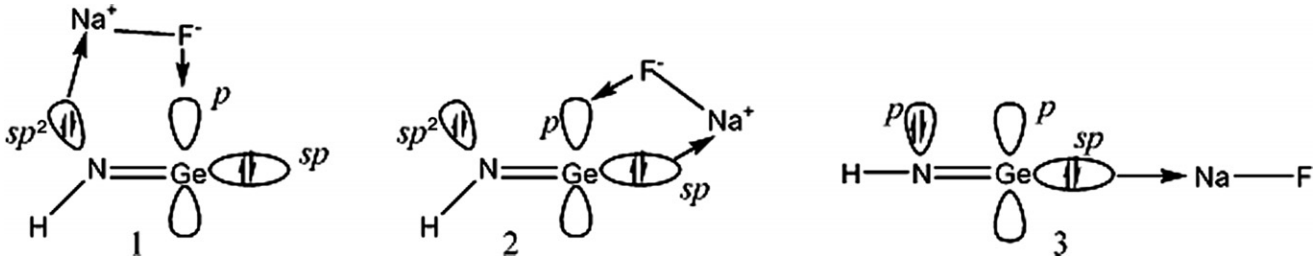

Fig. 3. Complexation process between HN=Ge: and NaF.

the hybridization of N atom has been changed from sp to sp^2 upon complexation. From the bond lengths, it can be seen that the N=Ge and Na–F bonds of complex **1** are weaker than those corresponding monomer, where both bonds are elongated by about 0.116 and 0.190 Å upon complexation, respectively. Overall, the stability of complex **1** has been enhanced through the donating of partial sp^2 electrons of N atom to the positive Na atom and the feedback of an electron lone pair of F atom to the sp-orbital of Ge atom, resulting in the formation of the electron circle of F → Ge → Na → F. As shown in Table 1, complex **1** has been stabilized by about 180.2 kJ/mol relative to those of monomers, which is the most stable one among the available complexes.

Complex **2** is characterized by a three-membered ring structure formed among Ge, Na, and F atoms, which is also in C_s symmetry. Similar to complex **1**, Ge and N atoms adopt sp and sp^2 hybridization, respectively. Complex **2** can be regarded as a product originating from the interaction between Na^+ and F^- in NaF and the sp occupied and p empty orbital in Ge, resulting in the formation of the donor–acceptor bonds of Ge → Na and F → Ge, respectively. Relative to the respective monomer, the N=Ge and Na–F bonds have been elongated by 0.048 and 0.101 Å upon complexation. Obviously, the three-membered ring structure has more ring strain compared with complex **1**. As a result, complex **2** has been stabilized by about 61.3 kJ/mol relative to the corresponding monomer.

As for complex **3**, it is characterized by a linear structure, which is in $C_{\infty v}$ symmetry. Here, as displayed in Fig. 3, both of the Ge and N atoms take sp hybridization and the complex **3** was formed when the electrons of the sp-occupied orbital in Ge migrate to Na^+. As a result, the N=Ge and Na–F bonds have been shortened and slightly elongated by about 0.014 and 0.003 Å upon complexation, respectively. As shown in Table 1, complex **3** has been only stabilized about 2.3 kJ/mol relative to the monomers of HN=Ge: and NaF.

Table 1
Relative energies of the complexes HN=GeNaF (in kJ/mol)

Species	HN=Ge: + NaF	1	2	3	4	5
B3LYP/6-311+G*	0.0	−180.2	−61.3	−2.3	−57.1	−2.2
MP2/6-311+G*	0.0	−159.6	−51.6	−4.9	−47.6	−4.0

3.2. Isomerization reactions of HN=GeNaF

As displayed in Fig. 2, two transition-state structures **4** and **5** have been located. Further IRC calculations suggest

that they are the true transition states for the isomerization reactions between complexes **1** and **2** and **2** and **3**, respectively. Vibration analysis calculations indicate that the unique imaginary frequencies of structures **4** and **5** are 55.91i and 18.96i cm^{-1}, respectively.

As presented in Table 1, the potential barrier from complex **1** to **2** is 123.1 kJ/mol and the reverse reaction is only 4.2 kJ/mol, implying the easy isomerization from the latter to the former. Similarly, the potential barrier from complex **2** to complex **3** is 59.1 kJ/mol and the reverse is only 0.1 kJ/mol. Thus, complex **1** should be the predominant form of HN=GeNaF in the gas phase thermodynamically and kinetically.

As mentioned above, we have also investigated the relevant HN=GeNaF species at the MP2/6-311+G* level of theory. As shown in Table 1, the validity of the B3LYP/6-311+G* level of theory can be confirmed from the consistent tendency between MP2 and B3LYP method. Thus, in the following study, complex **1** has been selected to investigate its insertion reactions with some small molecules R–H (R = F, OH, NH_2, and CH_3) at the B3LYP/6-311+G* level of theory.

3.3. Insertion reactions of HN=GeNaF and R–H

3.3.1. The structures and energies of the transition states

As mentioned above, complex **1** possesses C_s symmetry and there is an exposed space that can be attacked by nucleophiles or electrophiles under the Ge atom. Thus, the insertion reaction between HN=GeNaF and R–H should occur in this region.

As displayed in Fig. 4, the calculated transition states **TS1**–**TS4** in the insertion reactions have the similar structures. Here, the calculated unique imaginary frequencies are 1168.39i, 1349.19i, 1402.99i, and 1226.54i cm^{-1} for **TS1**, **TS2**, **TS3**, and **TS4**, respectively. Compared with the isolated HN=GeNaF, the bond distances between Ge and F^1 have been slightly shortened by 0.087, 0.057, 0.045, and 0.040 Å when R is F, OH, NH_2, and CH_3, respectively. On the other hand, the bond distance of R–H^2 has been elongated significantly to 1.404, 1.470, 1.570, and 1.830 Å, respectively. Thus, in these transition states, the R–H bond is to be broken and a new Ge–H^2 bond to be formed simultaneously. Correspondingly, relevant energy quantities about transition states have been summarized in Table 2.

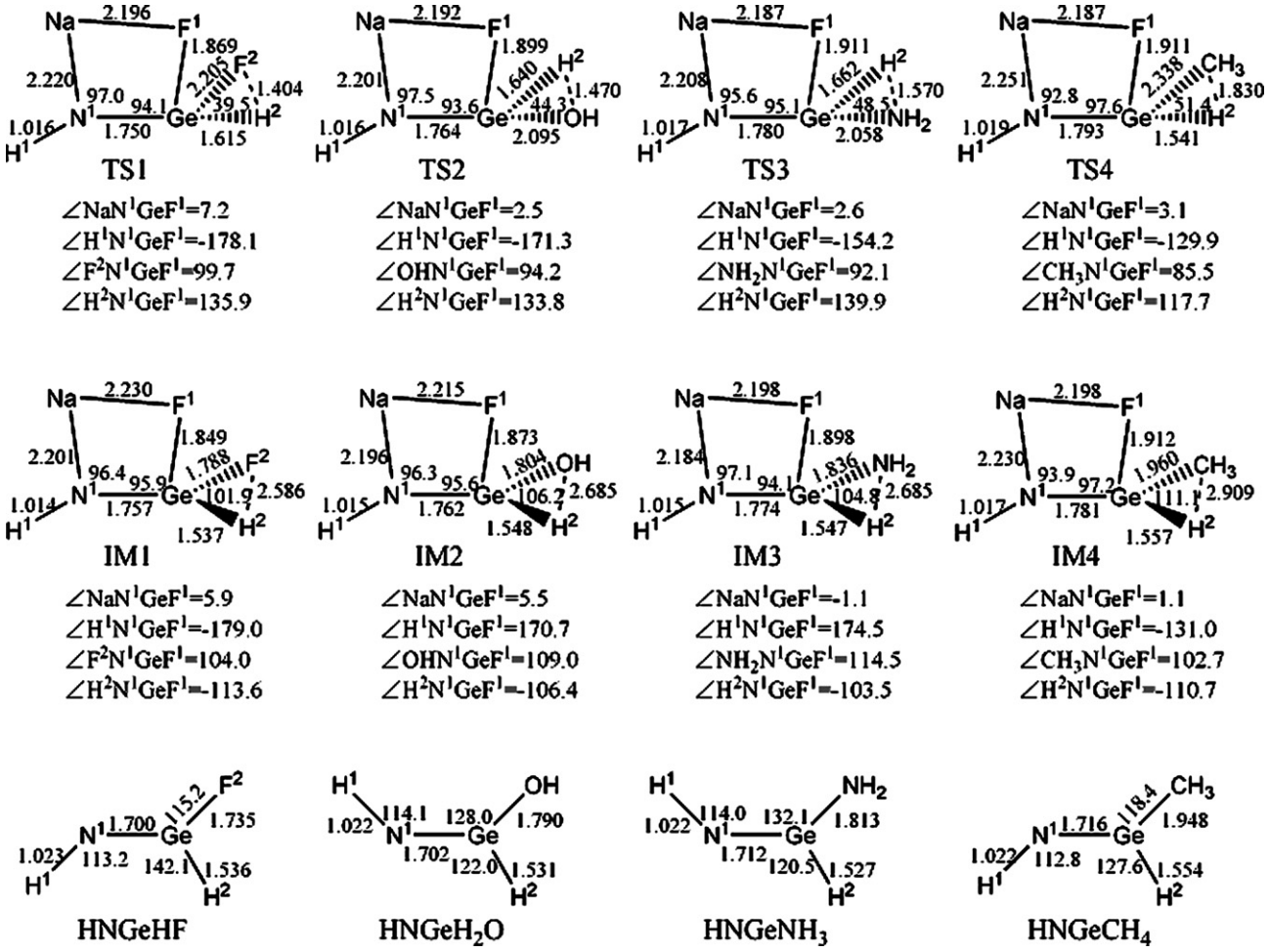

Fig. 4. Optimized structures of TSs, intermediates, and products, where the bond length and bond angel are in angstrom and degree, respectively.

Table 2
Relative energies of reactants, TSs, intermediates, and products in the insertion reactions for germylenoid and germylene with R–H (in kJ/mol)

Species	R = F	R = OH	R = NH_2	R = CH_3
HN=GeNaF + RH	0.0	0.0	0.0	0.0
TS (of HN=GeNaF + RH)	117.2	172.6	219.7	322.3
IM (of HN=GeNaF + RH)	−69.1	−20.7	12.2	59.3
HN=GeHR + NaF	185.0	208.1	224.4	266.9
HN=Ge: + RH	0.0	0.0	0.0	0.0
TS (of HN=Ge: + RH)	176.0	207.9	241.4	347.6
HN=GeHR	5.0	37.2	41.8	86.7

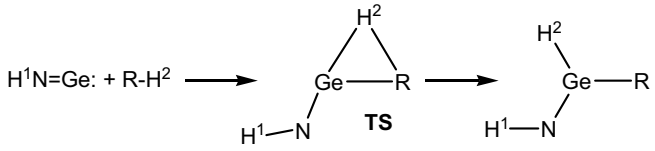

Scheme 1. The insertion reaction between HN=Ge: and R–H.

For the sake of comparison, we have also investigated the insertion reaction between germylene HN=Ge: and R–H (R = F, OH, NH_2, and CH_3) at the same calculation level, which can be denoted as the Scheme 1 and relevant energy quantities have been summarized in Table 2. Similarly, the insertion reaction proceeds first through a transition state (TS), where the barriers are 176.0 (R = F), 207.9 (R = OH), 241.4 (R = NH_2), and 347.6 kJ/mol (R = CH_3), respectively. Obviously, the barriers are higher 21.7–58.8 kJ/mol than those of reactions in the presence of NaF. Thus, as further mentioned below, the positive role of inorganic salts like NaF should be emphasized in the insertion reaction.

3.3.2. The structures and energies of the intermediates and products

As displayed in Fig. 4, four intermediates have been located in the insertion reactions. Obviously, all of them have similar structures. In detail, there are an approximate plane composed by the atoms of N^1, Ge, Na, and F^1, and the R and H^2 locate at the two sides of this plane. Compared with the isolated R–H, the R–H^2 bonds have been elongated significantly by about 1.658 (R = F), 1.721 (R = OH), 1.671 (R = NH_2), and 1.818 Å (R = CH_3), respectively, implying the broken of R–H^2 bond. At the same time, the distance between Ge and R atoms has been decreased significantly. For example, the corresponding bond lengths are 1.788 (R = F), 1.804 (R = OH), 1.836 (R = NH_2), and 1.960 Å (R = CH_3), respectively. At the same time, they have been shortened by 0.417, 0.291, 0.222, and 0.378 Å compared with the corresponding distance in the transition states, respectively, suggesting the formation of the new Ge–R bonds.

Further population analyses suggest that the net charges on Na (F^1) are 0.814 (−0.531), 0.791 (−0.536), 0.788 (−0.535), and 0.756 (−0.522) when R = F, OH, NH_2, and CH_3, respectively. Thus, the intermediates can be a strong ionic complex formed by HNGeHR, F^-, and Na^+ three fragments. With the increasing of the distance between HNGeHR and NaF fragments, these intermediates can be dissociated. To investigate this dissociation process, the potential energy curve for the **IM1** has been constructed along the distance between HNGeHR and NaF fragments. As displayed in Fig. 5, the energy of the system increases continuously before dissociation. Actually, no transition state has been located for this dissociation process to our best ability. Thus, the dissociation

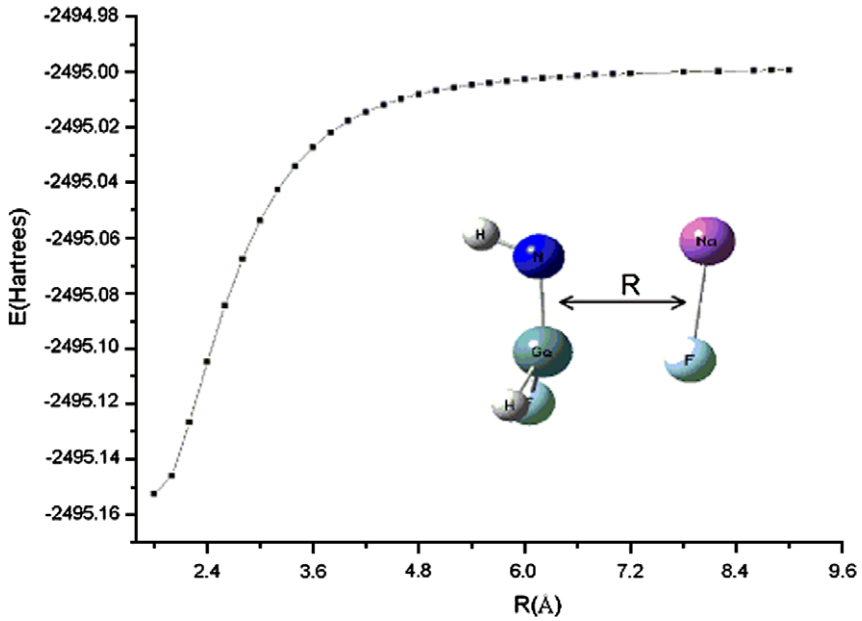

Fig. 5. Energy changes in dissociation process of IMI along with the distance between two fragments.

energy should be the barrier heights required for this dissociation process.

Additionally, as shown in Table 2, compared with the reactants, two intermediates have been stabilized by about 69.1 (R = F) and 20.7 (R = OH) kJ/mol. On the other hand, the other two complexes have been destabilized by 12.2 and 59.3 kJ/mol when R is NH_2 and CH_3, respectively. Correspondingly, the relative energies of the final products are 185.0, 208.1, 224.4 and 266.9 kJ/mol, suggesting that the whole reactions should be endothermic processes. As a result, the relative orders in reaction energies are as follows: R = F > R = OH > R = NH_2 > R = CH_3.

3.3.3. The mechanism of insertion reactions

Taking the process of inserting H–F bond as an example, IRC calculations have been performed on the basis of the calculated **TS1** to investigate the mechanism of the insertion process (see Fig. 6). Correspondingly, charge distributions for the selected atoms along the reaction coordinates have been presented in Table 3.

As shown in Table 3, the charges at the Ge and F^2 atoms increase gradually when the insertion reaction proceeds. At the same time, as displayed in Fig. 6, the distance between them decreases gradually, suggesting the formation of the Ge–F^2 bond. On the other hand, as for the bond lengths of H^2–F^2 and Ge–H^2, they increase and decrease with the proceeding of the reaction, implying the break of the former and the formation of the latter, respectively. Furthermore, a plot of the barrier heights (ΔE^*) versus the reaction enthalpy (ΔH) shows that ΔE^* varies linearly with ΔH for all the processes considered. Namely, as shown in Fig. 7, a linear correlation exists between ΔE^* and ΔH, i.e., $\Delta H = 0.397\Delta E^* + 138.54$, where the correlation coefficient is 0.9996. The point is similar to the insertion reactions between phosphinidenoid and R–H [39], manifesting the similarity between the phosphinidenoid and germylenoid. Thus, based on the existed correlation, one can predict the relative reaction activities qualitatively for the similar systems from the knowledge of reaction energies.

3.3.4. The comparisons of the insertion reactions

As shown in Table 2, the calculated barrier heights are 117.2, 172.6, 219.7, and 322.3 kJ/mol for the four different inserting reactions of R = F, OH, NH_2, and CH_3, respectively, exhibiting their different reactivities. Correspondingly, the calculated reaction energies are 185.0, 208.1, 224.4, and 266.9 kJ/mol, respectively. Thus, from the thermodynamic and kinetic viewpoints, the insertion reactions should occur easily in the order of H–F > H–OH > H–

Table 3
Population analyses for the selected atoms in TS1 along with the reaction coordinates

RX.COORD	Ge	F^2	H^2
−0.6	0.533	−0.268	0.281
−0.5	0.556	−0.290	0.270
−0.4	0.582	−0.314	0.260
−0.3	0.608	−0.339	0.250
−0.2	0.630	−0.363	0.240
−0.1	0.657	−0.389	0.231
0.0	0.694	−0.421	0.219
0.1	0.728	−0.451	0.208
0.2	0.751	−0.469	0.201
0.3	0.773	−0.482	0.195
0.4	0.792	−0.499	0.187
0.5	0.811	−0.512	0.180
0.6	0.829	−0.522	0.178

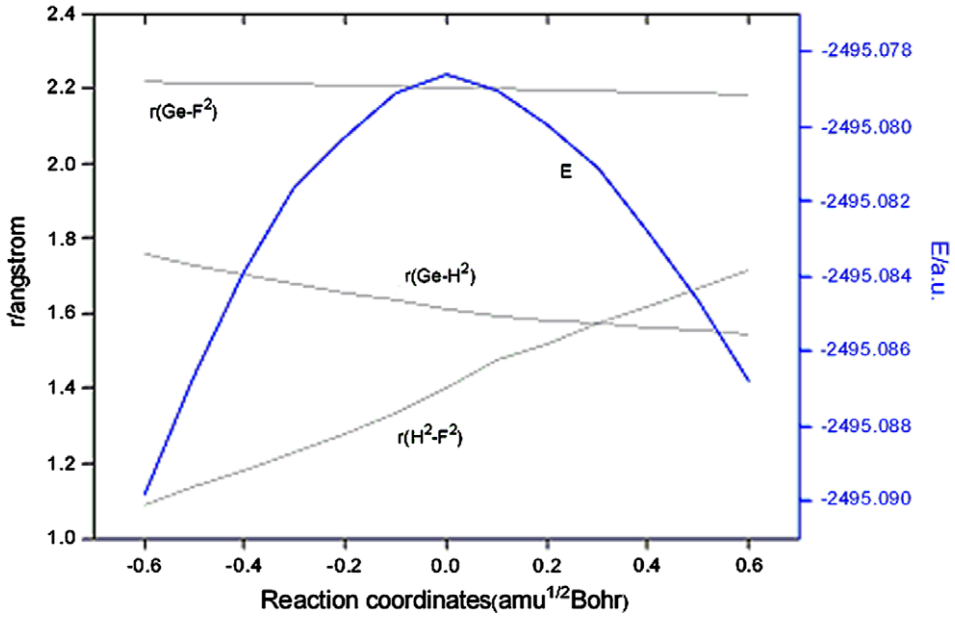

Fig. 6. The selected bond lengths and energy changes along the reaction coordinates.

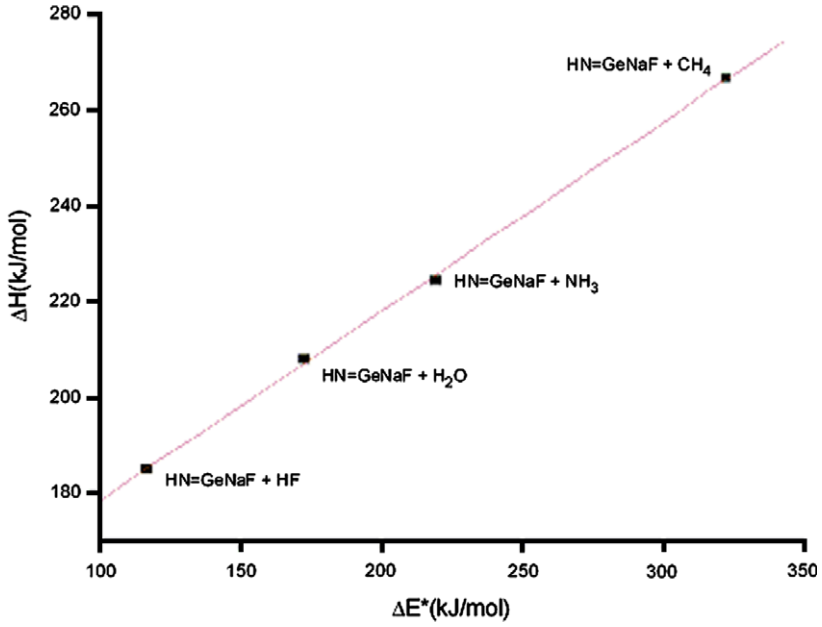

Fig. 7. The barrier height (ΔE^{*}) vs. the reaction enthalpy (ΔH) for the insertion of HN=GeNaF with R–H (R = F, OH, NH_2, CH_3).

NH_2 > H–CH_3 under the same condition. This point is also consistent with the calculated positive charges on the H atoms of the electrophiles, where the charges on the H atoms are 0.417, 0.369, 0.349, and 0.232 in HF, H_2O, NH_3, and CH_4, respectively. However, the relative activity is almost reversed if the negative charges on the R atoms of the nucleophiles are considered. Here, the charges on the R atom are −0.417, −0.739, −1.048, and −0.931 in HF, H_2O, NH_3, and CH_4, respectively. Thus, it seems that the insertion reactions should be predominated by the electrophiles attack.

Compared with H_2GeNaF and R–H [30], the insertion reaction of HN=GeNaF and R–H is more difficult. For example, the barrier heights in the present insertion reaction are higher 65.2, 50.6, 35.7, and 65.3 kJ/mol than those in the insertion reaction of H_2GeNaF and R–H when R is F, OH, NH_2, and CH_3, respectively. Correspondingly, as far as the reaction energies, the present results are also higher 228.0, 212.1, 203.4, and 215.9 kJ/mol than those in the insertion reaction of H_2GeNaF and R–H, respectively. Thus, from the kinetic and thermodynamic viewpoints, the insertion reaction of H_2GeNaF into R–H should occur easily than that of HN=GeNaF into R–H.

To get more insights into the reactive activity of the insertion reactions upon halogen substitution, we have also investigated the insertion reaction of germylenoid of X′N=GeNaF (X′ = H, F, Cl, Br) into R–H. Taking the insertion reaction into HF as an example, as shown in Table 4, both the barrier heights and reaction energies have been increased more or less, suggesting the decrease of the reactivity upon halogen substitution. At the same time, the halogen substituted cases have a similar reaction activity, which can be reflected from their similar barrier heights and reaction energies.

Table 4
Relative energies of reactants, TSs, intermediates, and products in the insertion reactions for germylenoid X′N=GeNaF into HF (in kJ/mol)

Species	X′ = H	X′ = F	X′ = Cl	X′ = Br
X′N=GeNaF[1] + HF[2]	0.0	0.0	0.0	0.0
TS	117.2	133.5	133.2	132.6
IM	−69.1	−49.3	−52.4	−53.9
X′N=GeHF[2] + NaF[1]	185.0	198.8	206.1	202.0

Table 5
Relative energies of reactants, TSs, intermediates, and products in the insertion reactions for germylenoid HN=GeMX into H–F (in kJ/mol)

Species	MX = not available	MX = NaF	MX = LiF	MX = NaCl	MX = LiCl
HN=GeMX + HF	0.0	0.0	0.0	0.0	0.0
TS	176.0	117.2	128.0	124.5	133.5
IM	–	−69.1	−60.5	−58.4	−52.7
HN=GeHF + MX	5.0	185.0	231.1	127.9	142.9

3.3.5. The influences of the inorganic salts in the insertion reactions

To investigate the role of different inorganic salts in the insertion reaction, the LiF, NaCl, and LiCl have been employed for comparison with NaF. Taking the insertion reaction into H–F as an example, as shown in Table 5, the barrier height has been reduced by about 42.5–58.8 kJ/mol in the presence of various inorganic salts, implying the positive role of the introduction of inorganic salts. Moreover, different inorganic salts have different influences on the reaction activity. For example, the barrier heights for the insertion reactions containing Na and F atoms are lower than those containing Li and Cl atoms, respectively. As a result, the positive role of NaF is much clearer than other inorganic salts in the present study.

4. Conclusions

In the present study, the geometries and isomerization of unsaturated germylenoid HN=GeNaF as well as its insertion reactions with R–H (R = F, OH, NH_2, CH_3) have been systematically investigated employing the B3LYP density functional method. Three stable complexes of HN=GeNaF have been located and the most stable one is characterized by a four-membered ring structure. The barrier heights of the four insertion reactions are 117.2, 172.6, 219.7, and 322.3 kJ/mol at the B3LYP/6-311+G* level of theory, respectively. All the mechanisms of the four reactions are identical to each other, i.e., an intermediate has been formed first during the insertion reaction. Then, the intermediate could dissociate into the substituted germylene (HN=GeHR) and NaF with a barrier corresponding to their corresponding dissociation energies. As a result, the relative reactivity among the four insertion reactions should be as follows: H–F > H–OH > H–NH_2 > H–CH_3. The reaction activity of the insertion reaction of imine germylene HN=Ge: has been enhanced significantly upon introductions of various inorganic salts. Compared with the insertion reaction of H_2GeNaF into R–H, imine germylenoid HN=GeNaF has lower reaction activity and is more difficult to insert the R–H bond. Additionally, the halogen substitution effects on the reaction activity have also been discussed. Hopefully, the present results are expected to fill a void in the available data for the study of the interactions between the unsaturated germylenoid and the molecules possessing the R–H characteristics.

Acknowledgements

This work is supported by the Scientific Research Foundation of Jinan University (XKY0709 and XJJ07045). We are highly grateful to the reviewer for his excellent suggestions to improve the presentation of the results.

References

[1] A.C. Filippou, J.G. Winter, G. kohn, J. Organomet. Chem. 544 (1997) 225.
[2] A.C. Filippou, P. Portius, J.G. Winter, J. Organomet. Chem. 628 (2001) 11.
[3] H. Ohgaki, W. Ando, J. Organomet. Chem. 521 (1996) 387.
[4] U. Anandhi, R. Paul, Inorg. Chim. Acta 359 (2006) 3521.
[5] B. Pampuch, W. Saak, M. Weidenbruch, J. Organomet. Chem. 691 (2006) 3540.
[6] S. Shoda, S. Iwata, K. Yajima, Tetrahedron 53 (1997) 15281.
[7] T. Iwamoto, H. Masuda, S. Ishida, J. Organomet. Chem. 689 (2004) 1337.
[8] K. Olaf, L. Peter, H. Joachim, Polyhedron 20 (2001) 2215.
[9] B. Eric, M. Stephane, H. Nancy, G. Heinz, J. Organomet. Chem. 691 (2006) 5619.
[10] C. Isobe, H. Cho, J.E. Sewell, Surf. Sci. 295 (1993) 117.
[11] W. Du, L.A. Keeling, C.M. Greenlief, J. Vac. Sci. Technol. A 12 (1994) 2281.
[12] C.G. Newman, J. Dzarnoski, M.A. Ring, Int. J. Chem. Kinet. 12 (1980) 661.
[13] W.A. Hermann, R.S. Grev, H.F. Schdfer, Angew. Chem. 104 (1992) 1489.
[14] N. Victor, I. Khrustalev, J. Organomet. Chem. 691 (2006) 1056.
[15] T. Shinobu, T. Hiromasa, K. Eunsang, M. Shigeki, S. Kenkichi, J. Organomet. Chem. 691 (2006) 595.
[16] R. Becerra, S.E. Boganov, M.P. Egorov, Chem. Phys. Lett. 260 (1996) 433.
[17] B. Rosa, P.E. Mikhail, I.V. Krylova, Chem. Phys. Lett. 351 (2000) 47.
[18] A. Ulan, D.K. Keith, D.L. Warren, Chem. Phys. Lett. 319 (2000) 529.
[19] A. Ulan, A.T. Neil, D.K. Keith, D.L. Warren, Chem. Phys. Lett. 299 (1999) 291.
[20] B. Rosa, W. Robin, J. Organomet. Chem. 636 (2001) 49.
[21] J. Satgi, Pure Appl. Chem. 56 (1984) 137.
[22] B. Rivière, D. Monique, J. Organomet. Chem. 595 (2000) 153.
[23] N. Tokitoh, K. Kishikawa, R. Okazaki, Polyhedron 21 (2002) 563.
[24] Z.Y. Geng, Y.C. Wang, H.Q. Wang, Acta Phys. Chim. Sin. 20 (2004) 1417.
[25] E. Broclawika, A.B. Janiszewska, J. Mole. Struc. (Theochem) 531 (2000) 241.
[26] R. Fang, X.H. Zhang, Z.Y. Geng, J. Mole. Struc. (Theochem) 761 (2006) 53.
[27] C.H. Lai, M.D. Su, S.Y. Chu, Chem. Commun. (2001) 1120.
[28] D.Q. Lei, P.P. Gaspar, Polyhedron 10 (1991) 1221.
[29] H.Y. Qiu, W.Y. Ma, G.B. Li, C.H. Deng, Chin. Chem. Lett. 10 (1999) 511.
[30] X.J. Tan, L. Ping, X.L. Yang, Int. J. Quantum Chem. 106 (2006) 1902.
[31] W.Z. Li, J.B. Cheng, B.A. Gong, J. Organomet. Chem. 691 (2006) 5984.
[32] N.C. Norman, Polyhedron 12 (1993) 2431.
[33] S. Foucat, T. Pigot, G.P. Guillouzo, S. Mazières, H. Lavayssière, Eur. J. Inorg. Chem. 7 (1999) 1151.
[34] S. Foucat, T. Pigot, G. Pfister-Guillouzo, Organometallics 18 (1999) 5322.
[35] P. Jutzi, Angew. Chem., Int. Ed. 39 (2000) 3797.
[36] Y. Apeloig, K. Albrecht, J. Am. Chem. Soc. 117 (1995) 7263.
[37] S.G. He, B.S. Tackett, D.J. Clouthier, J. Chem. Phys. 121 (2004) 257.
[38] C.W. Lee, T. Yang, R.G. Parr, Phys. Rev. B 37 (1988) 785.
[39] X.J. Tan, W.H. Wang, P. Li, X.L. Yang, G.X. Zheng, Theor. Chem. Acc. 118 (2007) 357.
[40] M.J. Frisch, et al., GAUSSIAN 98, Gaussian Inc., Pittsburgh, PA, 1998.